

Channel competition in dissociation of ammonia clusters ($n \leq 5$) induced by femtosecond laser fields

Tao Yang(杨涛), Xinyu Zhang(张馨予), Xing Li(李兴), Wankai Li(李万凯), Menghao Wei(卫孟昊), Dongdong Zhang(张栋栋), Lanhai He(赫兰海), and Dajun Ding(丁大军)

Citation: Chin. Phys. B, 2025, 34 (**3**): 033302. DOI: 10.1088/1674-1056/ada552
Journal homepage: http://cpb.iphy.ac.cn; http://iopscience.iop.org/cpb

What follows is a list of articles you may be interested in

Excitation and ionization of OCS molecules in strong UV and NIR laser fields

Huijun Shi(师慧军), Yang Liu(刘洋), Tian Sun(孙添), Hang Lv(吕航), and Haifeng Xu(徐海峰)
Chin. Phys. B, 2024, 33 (**7**): 073301. DOI: 10.1088/1674-1056/ad3035

Spectral attenuation of a 400-nm laser pulse propagating through a plasma filament induced by an intense femtosecond laser pulse

Quan-Jun Wang(王全军), Rao Chen(陈娆), Jia-Chen Zhao(赵家琛), Chun-Lin Sun(孙春霖), Xiao-Zhen Wang(王小珍), Jing-Jie Ding(丁晶洁), Zuo-Ye Liu(刘作业), Bi-Tao Hu(胡碧涛)
Chin. Phys. B, 2020, 29 (**1**): 013301. DOI: 10.1088/1674-1056/ab5a39

Effect of laser polarization on strong-field ionization and fragmentation of nitrous oxide molecules

Rui Wang(王瑞), Shi-Wen Zhang(张世文), Yang Liu(刘洋), Tian Sun(孙添), Hang Lv(吕航), Hai-Feng Xu(徐海峰)
Chin. Phys. B, 2019, 28 (**5**): 053301. DOI: 10.1088/1674-1056/28/5/053301

Identification of isomers and control of ionization and dissociation processes using dual-mass-spectrometer scheme and genetic algorithm optimization

Chen Zhou (陈洲), Tong Qiu-Nan (佟秋男), Zhang Cong-Cong (张丛丛), Hu Zhan (胡湛)
Chin. Phys. B, 2015, 24 (**4**): 043303. DOI: 10.1088/1674-1056/24/4/043303

Ellipticity-dependent ionization/dissociation of carbon dioxide in strong laser fields

Zhang Jun-Feng (张军峰), Ma Ri (马日), Zuo Wan-Long (左万龙), Lv Hang (吕航), Huang Hong-Wei (黄红卫), Xu Hai-Feng (徐海峰), Jin Ming-Xing (金明星), Ding Da-Jun (丁大军)
Chin. Phys. B, 2015, 24 (**3**): 033302. DOI: 10.1088/1674-1056/24/3/033302

Channel competition in dissociation of ammonia clusters ($n \leq 5$) induced by femtosecond laser fields

Tao Yang(杨涛)[1], Xinyu Zhang(张馨予)[2], Xing Li(李兴)[1,3], Wankai Li(李万凯)[1], Menghao Wei(卫孟昊)[1], Dongdong Zhang(张栋栋)[1], Lanhai He(赫兰海)[1,†], and Dajun Ding(丁大军)[1,‡]

[1] *Institute of Atomic and Molecular Physics, Jilin Provincial Key Laboratory of Applied Atomic and Molecular Spectroscopy, Jilin University, Changchun* 130012, *China*

[2] *Basic Courses Department, Tianjin Sino-German University of Applied Sciences, Tianjin* 300350, *China*

[3] *Institute of Atom Manufacturing, Nanjing University, Nanjing* 210093, *China*

(Received 23 December 2024; revised manuscript received 26 December 2024; accepted manuscript online 3 January 2025)

We investigated the ionization and dissociation processes of ammonia clusters ranging from dimer to pentamer induced by 800-nm femtosecond laser fields. Time-of-flight (TOF) mass spectra of the ammonia clusters were recorded over a range of laser intensities from 2.1×10^{12} W/cm^2 to 5.6×10^{12} W/cm^2. The protonated ion signals dominate the spectra, which is consistent with the stability of the geometric structures. The ionization and dissociation channels of ammonia clusters are discussed. The competition and switching among observed dissociation channels are revealed by analyzing the variations in the relative ionic yields of specific protonated and unprotonated clusters under different laser intensities. These results indicate that the ionization of the neutral multiple-ammonia units, produced through the dissociation of cluster ions, may start to contribute, as well as the additional processes to consume protonated ions and/or produce unprotonated ions induced by the femtosecond laser fields when the laser intensity is above $\sim 4\times10^{12}$ W/cm^2. These findings provide deeper insights into the ionization and dissociation dynamics in multi-photon ionization experiments involving ammonia clusters.

Keywords: ammonia cluster, ionization and dissociation, femtosecond laser

PACS: 33.80.Rv, 36.40.–c, 36.40.Wa

DOI: 10.1088/1674-1056/ada552 **CSTR:** 32038.14.CPB.ada552

1. Introduction

Significant efforts have been devoted to the study of molecular clusters for decades with particular emphasis on hydrogen bonds. Investigating hydrogen-bonding aggregations is essential for understanding fundamental effects such as solvation[1,2] and energetics on reaction dynamics.[3,4] Among hydrogen-bonding clusters, ammonia clusters have attracted special attention due to their significance in fields, e.g., physics, biology, and interplanetary chemistry.[5–9] Meanwhile, ammonia can also be used to synthesize nitride film and to make synthetic fibre.[10] In addition, ammonia clusters offer valuable insights into the behavior of dense states of matter governed by hydrogen-bonding interactions.[11–15] For instance, studying the behavior of ammonia clusters under physiological and pathological conditions can help elucidate the pathogenesis of diseases, offering a fundamental basis for diagnosis and treatment.[14,15]

Many research groups have extensively studied the structure stability of ammonia clusters for years. These investigations have explored spatial structures of neutral and protonated ammonia clusters and the corresponding infrared (IR) spectra, theoretically[4,16–19] and experimentally.[20–22] It is found that protonated cluster ions exhibit high stability. The time required for proton transfer depends on the distance between ammonia molecules within the cluster and the rate increases with cluster size, approaching saturation around $n = 5$.[19] Numerous studies consistently reveal that the primary ionic products of ammonia clusters are protonated cluster ions in the ionization and dissociation processes.[23–28] The formation of the proton-transferred products ($(NH_3)_{n-2}H_3NH^+\ldots NH_2$) in $(NH_3)_n^+$ ($n = 2$–4) have been discovered utilizing vacuum ultraviolet (VUV) photoionization and infrared predissociation spectroscopy (IRPDS-VUV-PI).[21,29] While in pump–probe experiments with dimer, it has been demonstrated that proton transfer occurs in a sequence of events, beginning with hydrogen transfer and subsequently followed by charge transfer and that the proton-transferred dimer reconfigures the ground state through relaxation of inverse proton transfer, resulting in dissociation into two NH_3 neutral fragments.[30] Recent studies employed coincidence measurement to identify proton transfer in multiply ionized dimer to tetramer ions during Coulomb explosions.[31,32] These investigations have provided more insights into the complex ionization and dissociation processes of ammonia clusters, which need further investigation to enhance our understanding.

This work investigates the ionization and dissociation

†Corresponding author. E-mail: helanhai@jlu.edu.cn

‡Corresponding author. E-mail: dajund@jlu.edu.cn

© 2025 Chinese Physical Society and IOP Publishing Ltd. All rights, including for text and data mining, AI training, and similar technologies, are reserved.

processes of ammonia clusters induced by femtosecond laser fields. Time-of-flight (TOF) mass spectra were experimentally measured at moderate laser intensities (10^{12} W/cm^2). Based on the observed relative yield ratios of specific protonated and unprotonated ions of dimer to pentamer under different laser intensities, we discuss the origin of these dissociation channels, and the corresponding competition and manipulation scenario under different laser intensities.

2. Experiment methods

The experimental setup is briefly described here, with detailed information available in our previous works.[33] Ammonia clusters are formed from a supersonically expanding molecular beam with a gas mixture containing 25% NH_3 in Ne, and a stagnation pressure of 0.05 MPa, which is introduced into the source chamber through a 150-μm diameter supersonic pulsed piezo-valve.[34] The valve operates with an opening time of 80 μs and a repetition rate of 100 Hz. The gas jet is then directed into a detection chamber through a 1 mm diameter skimmer. The linearly polarized (parallel to the detector) laser beam (800 nm, 50 fs), produced by chirped-pulse-amplified Ti:sapphire femtosecond laser (Libra HE, Coherent, Inc), is focused into the cluster beam using a spherical mirror with a 275-mm focal length, intersecting the center of the cluster beam. The radius of the beam waist before the focusing mirror is ∼4 mm, and the laser intensity can be varied from 2.1×10^{12} W/cm^2 to 5.6×10^{12} W/cm^2. The generated photoions travel approximately 500 mm in a velocity map imaging (VMI) spectrometer operating in TOF mode. The detection system consists of a pair of microchannel plates coupled with a P47 phosphor screen. A photomultiplier tube (PMT) converts the light signal from the phosphor screen into an electrical signal, which is then sent to the oscilloscope for processing. Finally, the signal is transferred to a computer for analysis.

3. Results and discussion

The TOF mass spectra of ammonia clusters triggered by 800-nm femtosecond laser have been measured, as shown in Fig. 1 partially. The cluster size distribution, ranging from monomeric ammonia to clusters containing up to 40 ammonia molecules, is roughly estimated based on the ionic distributions presented in Fig. 1(a). Based on the observed ionic populations, the average size of the ammonia clusters is estimated to be $\langle n\rangle \approx 6$. Therefore, the sizes of the ammonia clusters discussed in the present experiment are mainly $n \leq 5$. The spectra show predominant features of protonated cluster ions, besides monomeric ammonia ions, with some minor contributions from small unprotonated cluster ions. This is mainly attributed to the larger probability of unprotonated parent cations $(NH_3)_n^+$ undergoing dissociation along the cation potential energy surface in the laser fields, leading to protonated products $(NH_3)_{n-1}H^+$ which are more stable than that to unprotonated products.[35,36] In addition, the smaller fragmental ions NH_2^+ and NH^+ cannot be observed under the relatively low laser intensities, due to the high appearance energy.[37] A significant variation in the relative ionic yields from protonated dimers to pentamers under different laser intensities has been observed: at low laser intensities, these yields remain relatively consistent, but they progressively turn into a decreasing trend at high laser intensity, as shown in Figs. 1(b) and 1(c). This trend is consistent with the result reported by Castleman *et al.* using 266-nm nanosecond laser[25] and has been attributed to the increasing occurrence of substantial fragmentation with rising laser intensity. It is noted from the mass spectra that the protonated pentamer signal appears as a "step", indicating the magic number in ammonia cluster-size distributions,[25,26] consistent with previous studies.[35]

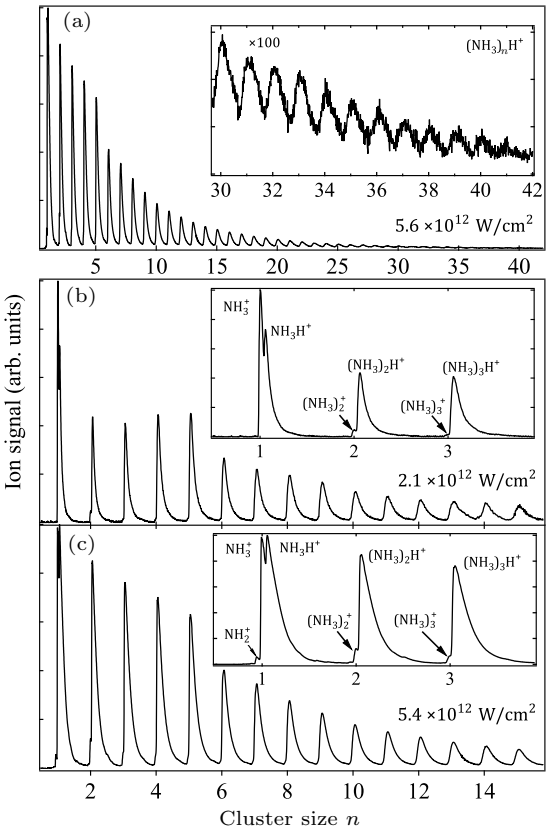


Fig. 1. The TOF mass spectra for $1 \leq n \leq 42$ (a) and $1 \leq n \leq 15$ [(b), (c)] of ammonia clusters under different laser intensities, wherein the insets show the zoomed-in views for $30 \leq n \leq 42$ (a), and $1 \leq n \leq 3$ [(b), (c)].

In the femtosecond laser field, unprotonated ammonia cluster ions can undergo proton transfer, forming a spatial structure with the $NH_4^+ \ldots NH_2$ core configuration.[29,38] Thus the protonated cluster ions can be formed through further losing NH_2. Figure 2 shows the spatial structure for the neutral clusters $(NH_3)_n$, unprotonated cations $(NH_3)_n^+$, and protonated cations $(NH_3)_nH^+$ for $n = 2$ and 3, calculated at MP2/6-311++g(d,p) level. Table 1 lists the obtained bond for all hydrogen bonds N...H and distances of nitrogen–nitrogen (NN)

within each cluster. The results show that the hydrogen bond lengths decrease from the neutral clusters to the cluster ions, as expected that the spatial structure of a cluster would shrink during the removal of an electron. Besides, it can be seen from Table 1 that the hydrogen bond lengths for protonated cluster ions are shorter than that for unprotonated ions, for example, the length of hydrogen bond is 2.260 Å and 1.693 Å for neutral and ionic dimer, respectively, while the length for the protonated dimer is 1.574 Å. The result indicates a more stable protonated cluster can be favorably formed after ionization, taking into account the dissociation energy of parents ions $(NH_3)_n^+$ $(n > 2)$ into protonated ions $(NH_3)_{n-1}H^+$ is higher relative to that into unprotonated ions $(NH_3)_{n-1}^+$, due to one photon energy of 800-nm laser ($h\nu = 1.55$ eV) is high enough to overcome these dissociation energy barriers (in the case of $(NH_3)_3^+$, the dissociation into $(NH_3)_2^+$ and $(NH_3)_2H^+$, the required energies are 0.36 eV and 0.7 eV, respectively[35,36,38]).

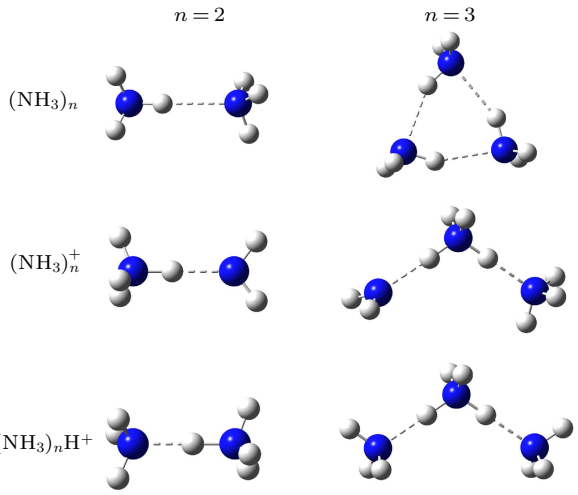


Fig. 2. Optimized geometrical structures of the neutral cluster, protonated cluster ion, and unprotonated cluster ion, for ammonia clusters with cluster sizes of $n = 2$–3 at the MP2/6-311++g(d,p) level. Dotted lines denote the hydrogen bonds between the atoms of the nitrogen (blue balls) and hydrogen (grey balls).

Table 1. The intermolecular NN distances and N...H hydrogen bond lengths in Angstroms (Å), of ammonia clusters.

	R(NN)		*R*(N...H)	
	Present work	Reference	Present work	Reference
$(NH_3)_2$	3.261	3.252[18]	2.260	2.262[38]
$(NH_3)_3$	3.173	3.172[18]	2.221	2.218[38]
$(NH_3)_2^+$	2.768	2.174[35]	1.693	1.692[38]
$(NH_3)_3^+$	2.876†	2.752[35]	1.720, 1.827	1.736,[35] 1.855[35]
$(NH_3)_2H^+$	2.694	2.706[35]	1.574	1.593[35]
$(NH_3)_3H^+$	2.818†	2.833[35]	1.750	1.769[35]

† The one in line with the hydrogen bond direction

To quantitatively analyze the variation in the ionic yields of ammonia clusters with laser intensity, we extracted the actual relative yields of several specific ionic species and presented them in Fig. 3 on a log–log scale. The ionic yields of protonated ammonia cluster for different sizes in Fig. 3(a) exhibit a dependence on laser intensity with a slop ≈ 4 for $n = 5$–10 in log–log diagrams, which suggests that the occurrence of the resonance with the excited $\widetilde{A}$ state[26,36,39] via the absorption of four 800-nm photons. While the fitted slop is ≈ 4.5 for the ammonia clusters with $n = 1$–4. This may be due to the dissociation of relatively large-sized protonated cluster ions (as further illustrated by Eq. (3) later). This is also consistent with the observed trend for the relative yield change from dimer to pentamer protonated ions with increasing laser intensity in Fig. 1. On the other hand, the ionic yields of unprotonated clusters show different dependence on laser intensity. In Fig. 3(b), though NH_3^+ increase with a slop about 4, the yields of $(NH_3)_2^+$ and $(NH_3)_3^+$ exhibit a faster growth tendency with increasing the laser intensity. In particular, these data show a bending at the laser intensity around 4×10^{12} W/cm^2, into two parts, with the fitted slopes being ~ 4 and 6 for the laser intensity below and above this laser intensity respectively. These unusual trends suggest complex ionization and fragmentation dynamics of ammonia clusters sensitive to laser intensity.

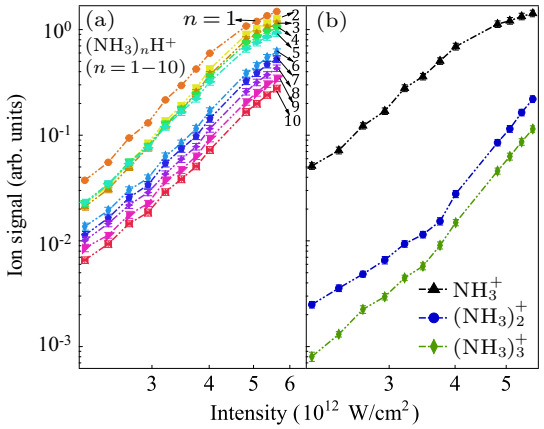


Fig. 3. Ionic yields as a function of laser intensity (log–log scale): (a) for protonated ions $(NH_3)_nH^+$ $(n = 1$–$10)$, and (b) for unprotonated ions $(NH_3)_n^+$ $(n = 1$–$3)$.

Considering the ammonia clusters interacted with femtosecond laser fields, the neutral clusters tend to undergo ionization followed by dissociation.[27] The first ionization energies[25,40] for $n = 1$–5 are 10.18 eV, 9.54 eV, 9.3 eV, 9.0 eV, and 8.7 eV, respectively. Firstly, the ionization process of the neutral species preferably occurs with a four-photon res-

onance via the intermediate state.[26,41] Afterward, it undergoes a three-photon or two-photon ionization process, e.g.,

$$(NH_3)_n + 4h\nu \rightarrow (NH_3)_n^* + 3h\nu \rightarrow (NH_3)_n^+ + e^-,$$

then, the ionic ammonia clusters may absorb another one 800-nm photon, leading to dissociation from two possible channels, producing unprotonated and protonated products,[27,42] as shown below:

$$(NH_3)_n^+ + h\nu \rightarrow (NH_3)_{n-m}^+ + mNH_3, \quad (1)$$

$$\rightarrow (NH_3)_{n-m}H^+ + (m-1)NH_3 + NH_2, \quad (2)$$

where $n \geq 2$, $m = 1, 2, \ldots, n-1$. In particular, once the protonated ammonia cluster ions are generated via the dissociation channel (2), they are more likely to undergo further fragmentation through molecular decay[38,43] assisted by laser fields, involving the loss of one or several neutral ammonia molecules,

$$(NH_3)_{n-m}H^+ \rightarrow (NH_3)_{n-m-a}H^+ + aNH_3, \quad (3)$$

where $a = 1, 2, \ldots, n-m-2$. These dissociation processes induced by femtosecond laser fields intrinsically differ from the nanosecond laser case. In the typical infrared femtosecond laser case,[26] the ionization of neutral clusters usually happens at the beginning with multiple probable ionization channels, followed by dissociation, while in the typical ultraviolet nanosecond laser case,[28,44] the hydrogen transfer of neutral within the clusters, producing neutral protonated clusters, is more likely to occur first, followed by ionization resulting in the protonated ionic products.

Furthermore, we extract the ratios of ionic yields for several specific protonated and unprotonated clusters originating from two distinct processes. These results demonstrate a competition between dissociation channels with varying laser intensities. In Fig. 4, the ratios of $(NH_3)_2H^+/(NH_3)_2^+$ and $(NH_3)_3H^+/(NH_3)_3^+$ in the beginning increase. However, as the laser intensity further increases from $\sim 4\times10^{12}$ W/cm^2, these ratios decrease threefold, while the ratios remain above one. These unprotonated clusters ions $(NH_3)_2^+$, $(NH_3)_3^+$, and protonated clusters ions $(NH_3)_2H^+$, $(NH_3)_3H^+$, originate primarily from channel (1) and channel (2) respectively.[38,45] We take the ratio $(NH_3)_3H^+/(NH_3)_3^+$ as an example. $(NH_3)_3^+$ is primarily produced either along with one ammonia unit through the dissociation of $(NH_3)_4^+$, or along with two ammonia units via the dissociation of $(NH_3)_5^+$.[35] $(NH_3)_3H^+$ is mainly produced either along with one NH_2 fragment through the dissociation of $(NH_3)_4^+$, or along with the loss of one NH_2 and one NH_3 fragments during the dissociation of $(NH_3)_5^+$.[38] Additionally, the relatively larger protonated ion products, e.g., $(NH_3)_4H^+$, are preferable to undergo further dissociation through channel (3) into smaller-sized protonated ions,[43] e.g., $(NH_3)_3H^+$, with increasing laser intensity. These processes synergistically lead to an increase of the protonated ions $(NH_3)_3H^+$, and the ratio of $(NH_3)_3H^+/(NH_3)_3^+$ under the low laser intensity. When the laser intensity is above $\sim 4\times10^{12}$ W/cm^2, the decreasing trend of the ratio implies that unprotonated ionic products are promoted rapidly, compared with the protonated ions. Taking into account the low dissociation energies of the cluster ions,[35,38] the neutral three-ammonia unit can be formed through three dissociation channels: the dissociation of $(NH_3)_4^+$ along with NH_3^+ product (1), the dissociation of $(NH_3)_5^+$ along with $(NH_3)H^+$ product (2), and the dissociation channel (3) of $(NH_3)_4H^+$ along with $(NH_3)H^+$ product (3). The typical timescale for these dissociation channels is within 100 fs,[46] these produced neutral ammonia units are very likely to be further ionized within the same femtosecond laser pulse, contributing to unprotonated cluster ionic products, resulting in an increase of the unprotonated ions $(NH_3)_3^+$. Meanwhile, the femtosecond laser fields may induce additional processes to consume $(NH_3)_3H^+$ and/or produce $(NH_3)_3^+$, leading to the decrease in the ratio $(NH_3)_3H^+/(NH_3)_3^+$, e.g., the much greater degree of fragmentation of the protonated cluster ions $(NH_3)_3H^+$,[25] and the ionization of the neutral ammonia clusters $(NH_3)_3$ without further dissociation, via the absorption of more than the minimum photon numbers required for ionization.[28] These results highlight the complex competition between the dissociation channels of multiple-sized ammonia clusters induced by femtosecond laser fields at moderate laser intensities (10^{12} W/cm^2). The database obtained in this work facilitates further investigations based on advanced theoretical models or sophisticated experimental approaches.

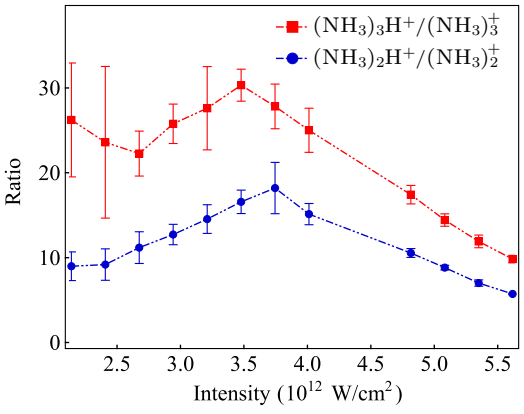


Fig. 4. The ratios between the protonated and unprotonated cluster ions, red squares for $(NH_3)_3H^+$ to $(NH_3)_3^+$, and blue circles for $(NH_3)_2H^+$ to $(NH_3)_2^+$.

4. Conclusion

In summary, we investigated the ionization followed by the dissociation processes of ammonia clusters, from dimers to pentamers, induced by 800-nm femtosecond laser fields. The TOF spectra with varying laser intensities exhibit pronounced

protonated ion signals, which are attributed to their relatively high structural stability with the $NH_4^+...NH_2$ core configuration. The ionic yield ratios of $(NH_3)_3H^+$ to $(NH_3)_3^+$ and $(NH_3)_2H^+$ to $(NH_3)_2^+$ under different laser intensities, indicate the competition between different dissociation channels. When the laser intensity is above $\sim 4 \times 10^{12}$ W/cm^2, the neutral multiple-ammonia units, produced from the dissociation of cluster ions, can be further ionized, as well as the additional processes to consume protonated ions and/or produce unprotonated ions induced by the femtosecond laser fields, via the much greater degree of fragmentation of the protonated cluster ion and/or the absorption of more than the minimum photon numbers required for ionization. These complex dissociation processes lead to the change in the ratios with laser intensity. These findings provide deeper insights into the ionization and dissociation dynamics of ammonia clusters, suggesting the laser intensity may serve as a potential control for manipulating ionic products, possibly extending this approach to other hydrogen-bonded clusters, such as water or methanol clusters.

Acknowledgement

Project supported by the National Natural Science Foundation of China (Grant Nos. 92261201, 12134005, and 12334011).

References

[1] Hush N S and Reimers J R 2000 *Chem. Rev.* **100** 775
[2] Baranyi B and Turi L 2019 *J. Chem. Phys.* **151** 204304
[3] Custelcean R and Jackson J E 2001 *Chem. Rev.* **101** 1963
[4] Malloum A, Fifen J J and Conradie J 2020 *J. Comput. Chem.* **41** 21
[5] Penner R C, Andersen E S, Jensen J L, Kantcheva A K, Bublitz M, Nissen P, Rasmussen A MH, Svane K L, Hammer B, Rezazadegan R, Chr Nielsen N, Nielsen J T and Andersen J E 2014 *Nat. Commun.* **5** 5803
[6] Perrin C L and Nielson J B 1997 *Annu. Rev. Phys. Chem.* **48** 511
[7] Wang Y J, Liu M Y and Gao J L 2020 *Proc. Natl. Acad. Sci. USA* **117** 13967
[8] Dantus M 2024 *Science* **385** eadk1833
[9] Larsson M and Geppert W D and Nyman G 2012 *Rep. Prog. Phys.* **75** 066901
[10] Briggs N, Preciado M I, Lu Y F, Wang K, Leach J, Li X F, Xiao K, Subramanian S, Wang B M, Haque A, Sinnott S and Robinson J A 2018 *Nanotechnology* **29** 47LT02
[11] Oostenrijk B, Walsh N, Laksman J, Månsson E P, Grunewald C, Sorensen S L and Gisselbrecht M 2018 *Phys. Chem. Chem. Phys.* **20** 932
[12] Michiels R, LaForge A C, Bohlen M, Callegari C, Clark A, von Conta A, Coreno M, Fraia D M, Drabbels M, Finetti P, Huppert M, Oliver V, Plekan O, Prince K C, Stranges S, Svoboda V, Wörner J H and Stienkemeier F 2020 *Phys. Chem. Chem. Phys.* **22** 7828
[13] Hu Z, Jin M X, Xu X S, Cheng X H and Ding D J 2006 *Front. Phys. China* **1** 275
[14] Raja G, Gupta H, Gebru Y A, Youn G S, Choi Y R, Kim H S, Yoon S J, Kim D J, Kim T J and Suk K T 2021 *Int. J. Mol. Sci.* **22** 1160
[15] Atluri D K, Prakash R and Mullen K D 2011 *J. Clin. Exp. Hepatol.* **1** 77
[16] Tono K, Bito K, Kondoh H, Ohta T and Tsukiyama K 2006 *J. Chem. Phys.* **125** 224305
[17] Malloum A, Fifen J J and Conradie J 2018 *J. Chem. Phys.* **149** 024304
[18] Wang B, Hou P G, Cai Y M, Guo Z D, Han D D, Gao Y and Zhao L 2020 *ACS Omega* **5** 31724
[19] Tachikawa H 2020 *J. Phys. Chem. A* **124** 1903
[20] Malloum A, Fifen J J, Dhaouadi Z, Nana Engo S G and Jaidane N E 2017 *J. Chem. Phys.* **146** 044305
[21] Katada M, Shishido R and Fujii A 2014 *Phys. Chem. Chem. Phys.* **16** 7595
[22] Zhang B B, Yang S, Huang Q R, Jiang S K, Chen R J, Yang X M, Zhang D H, Zhang Z J, Kuo J L and Jiang L 2021 *CCS Chem.* **3** 829
[23] Echt O, Morgan S, Dao P D, Stanley R J and Castleman A W Jr 1984 *Ber. Bunsenges. Phys. Chem.* **88** 217
[24] Shinohara H and Nishi N 1987 *Chem. Phys. Lett.* **141** 292
[25] Castleman A W Jr, Tzeng W B, Wei S and Morgan S 1990 *J. Chem. Soc. Faraday Trans.* **86** 2417
[26] Wei S, Purnell J, Buzza S A, Stanley R J and Castleman A W Jr 1992 *J. Chem. Phys.* **97** 9480
[27] Xia P, Lyktey M Y M and Garvey J F 1994 *J. Chem. Phys.* **101** 10193
[28] Buzza S A, Wei S, Purnell J and Castleman A W Jr 1995 *J. Chem. Phys.* **102** 4832
[29] Hachiya M, Matsuda Y, Suhara K, Mikami N and Fujii A 2008 *J. Chem. Phys.* **129** 094306
[30] Horke D A, Watts H M, Smith A D, Jager E, Springate E, Alexander O, Cacho C, Chapman R T and Minns R S 2016 *Phys. Rev. Lett.* **117** 163002
[31] Zhou J Q, Belina M, Jia S K, Xue X R, Hao X T, Ren X G and Slavíček P 2022 *J. Phys. Chem. Lett.* **13** 10603
[32] Zhang X Y, Zhao X N, Liu H, Yin Z Y, Zhao X G, Ma P, Li X K, Wang C C, Wang Q X, Luo S Z and Ding D J 2024 *Phys. Rev. A* **109** 023112
[33] He L H, Pan Y, Yang Y J, Luo S Z, Lu C J, Zhao H F, Li D X, Song L L, Stolte S, Ding D J and Roeterdink W G 2016 *Chem. Phys. Lett.* **665** 141
[34] Irimia D, Dobrikov D, Kortekaas D, Voet H, van den Ende D A, Groen W A and Janssen M H M 2009 *Rev. Sci. Instrum.* **80** 113303
[35] Park J K 2000 *J. Phys. Chem. A* **104** 5093
[36] Snyder E M, Purnell J, Wei S, Buzza S A and Castleman A W Jr 1996 *Chem. Phys.* **207** 355
[37] Dixon D A, Feller D and Peterson K A 2001 *J. Chem. Phys.* **115** 2576
[38] Yuan B, Shin J W and Bernstein E R 2016 *J. Chem. Phys.* **144** 144315
[39] Song L L, Sun Y N, Wang Y H, Wang X C, He L H, Luo S Z, Hu W H, Tong Q N and Ding D J 2019 *Chin. Phys. B* **28** 063201
[40] Reiser G and Habenicht W and Müller-Dethlefs K 1993 *J. Chem. Phys.* **98** 8462
[41] Okai N, Takahata A, Morita M, Nonose S and Fuke K 2004 *J. Phys. Chem. A* **108** 727
[42] Dong F, Heinbuch S, Rocca J J and Bernstein E R 2006 *J. Chem. Phys.* **124** 224319
[43] Echt O, Dao P D, Morgan S and Castleman A W Jr 1985 *J. Chem. Phys.* **82** 4076
[44] Li L B and Wang X Y 1999 *Chem. Phys. Lett.* **304** 60
[45] Misaizu F, Houston P L, Nishi N, Shinohara H, Kondow T and Kinoshita M 1993 *J. Chem. Phys.* **98** 336
[46] Shinohara H, Nishi N and Washida N 1985 *J. Chem. Phys.* **83** 1939